Systemic Blockade of Sialylation in Mice with a Global Inhibitor of Sialyltransferases*[S]

Matthew S. Macauley[‡1], **Britni M. Arlian**[‡1], **Cory D. Rillahan**[‡§], **Poh-Choo Pang**[¶], **Nikki Bortell**[||],
Maria Cecilia G. Marcondes[||], **Stuart M. Haslam**[¶], **Anne Dell**[¶], and **James C. Paulson**[‡2]

From the ‡*Departments of Cell and Molecular Biology, Chemical Physiology, and Immunology and Microbial Science and the* ||*Department of Molecular and Cellular Neuroscience, The Scripps Research Institute, La, Jolla, California 92037, the* §*Division of Cancer Biology and Genetics, Memorial Sloan-Kettering Cancer Center, New York, New York 10065, and the* ¶*Department of Life Sciences, Faculty of Natural Sciences, Imperial College London, London SW7 2AZ, United Kingdom*

Background: *In vivo* pharmacological inhibition of sialyltransferases has, to date, not been possible.
Results: 3F-NeuAc acts as a global sialyltransferase inhibitor in mice and causes kidney and liver dysfunction.
Conclusion: Sialoside expression can be modulated *in vivo* with a sialyltransferase inhibitor.
Significance: Pharmacological blockade of sialoside expression will be an important tool for future exploration of sialic acid in health and disease.

Sialic acid terminates glycans of glycoproteins and glycolipids that play numerous biological roles in health and disease. Although genetic tools are available for interrogating the effects of decreased or abolished sialoside expression in mice, pharmacological inhibition of the sialyltransferase family has, to date, not been possible. We have recently shown that a sialic acid analog, 2,4,7,8,9-pentaacetyl-3F$_{ax}$-Neu5Ac-CO$_2$Me (3F-NeuAc), added to the media of cultured cells shuts down sialylation by a mechanism involving its intracellular conversion to CMP-3F-NeuAc, a competitive inhibitor of all sialyltransferases. Here we show that administering 3F-NeuAc to mice dramatically decreases sialylated glycans in cells of all tissues tested, including blood, spleen, liver, brain, lung, heart, kidney, and testes. A single dose results in greatly decreased sialoside expression for over 7 weeks in some tissues. Although blockade of sialylation with 3F-NeuAc does not affect viability of cultured cells, its use *in vivo* has a deleterious "on target" effect on liver and kidney function. After administration of 3F-NeuAc, liver enzymes in the blood are dramatically altered, and mice develop proteinuria concomitant with dramatic loss of sialic acid in the glomeruli within 4 days, leading to irreversible kidney dysfunction and failure to thrive. These results confirm a critical role for sialosides in liver and kidney function and document the feasibility of pharmacological inhibition of sialyltransferases for *in vivo* modulation of sialoside expression.

Sialic acid (*N*-acetylneuraminic acid; NeuAc)[3] is a nine-carbon sugar that terminates complex cell surface glycans and is unique to vertebrates and certain bacteria (1). Cell surface sialosides on higher eukaryotic cells have been implicated in highly diverse physiological processes (2). For example, as ligands for sialic acid binding proteins, sialosides mediate cellular homing and adhesion of leukocytes (3), modulation of immune responses (4), and adhesion of viral and bacterial pathogens to host cells (5). Sialosides also play key roles in fertilization (6), brain development (7), muscular function (8), and kidney function (9). Genetic deficiency in the cellular biosynthesis of sialic acid results in lethality during embryonic development in mice (10), highlighting the importance of sialic acid at the organismal level. Conversely, hypersialylation is a hallmark of many cancer cell types, and up-regulation of cell surface sialic acid is proposed to play a role in cancer progression through a variety of mechanisms (11).

In higher eukaryotes, sialic acid is linked to the underlying glycan via an α-glycosidic linkage to the 3′ or 6′ position of a galactose residue, the 6′ position of an *N*-acetylgalactosamine residue, or the 8′ position of another sialic acid residue. These protein- or lipid-linked α2,3-, α2,6-, and α2,8-sialosides are generated enzymatically by the cumulative actions of 20 different sialyltransferases, which all use CMP-NeuAc as their common donor substrate (12). Importantly, because of differences in acceptor substrate specificity and gene expression patterns of these related enzymes, cells and tissues display unique sialoside structures, which can have important functional consequences (13–15). Studies examining sialyltransferase-deficient mice, for instance, have shed light on some of the important biological roles played by sialosides in the immune response (16–22), brain (23–27), and blood/liver (19, 28).

[3] The abbreviations used are: NeuAc, 5-acetyl-neuraminic acid; 3F-NeuAc, 2,4,7,8,9-pentaacetyl-3F$_{ax}$-Neu5Ac-CO$_2$Me; NeuGc, 5-glycolyl-neuraminic acid; LacNAc, galactose(1,4)α-*N*-acetylglucosamine; ManNAc, *N*-acetylmannosamine; Fuc, Fucose; SNA, *S. nigra* agglutinin; PNA, peanut agglutinin; MAA, *M. amurensis* agglutinin.

In Vivo Use of a Global Sialyltransferase Inhibitor

In principle, use of small molecule inhibitors of sialyltransferases offers a complementary approach to genetic methods for studying the *in vivo* role(s) of sialosides. In particular, they address the concern about genetic deficiencies on development and can assess the kinetics for the onset and reversibility of an observed phenotype with control of administration and withdrawal of inhibitor. The majority of sialyltransferase inhibitors developed to date are not cell-permeable, and hence, no sialyltransferase inhibitor has been used to alter sialoside expression levels *in vivo*. Recently, we developed a global inhibitor of the sialyltransferase family that is highly effective at inhibiting sialoside expression in cultured cells (29). Using a pro-drug approach, peracetylated $3F_{ax}$-NeuAc (3F-NeuAc) is efficiently taken up by cells, deacetylated, and transformed into CMP-3F-NeuAc. CMP-3F-NeuAc is a very poor substrate for sialyltransferases because of the electron-withdrawing effect of the fluorine atom that destabilizes the proposed oxocarbenium ion-like transition state, effectively acting as a competitive inhibitor (30, 31). Furthermore, CMP-3F-NeuAc accumulates to high levels in the cell and, because of the metabolic feedback loops, leads to the depletion of endogenous CMP-NeuAc (29). It is noteworthy that although blockade of sialylation with 3F-NeuAc did not alter the viability of cultured cells (29), genetic disruption of sialic acid biosynthesis is embryonically lethal in mice (10). In contrast, transgenic mice with partial disruption of sialic acid biosynthesis (32–34) or deficiencies in expression of individual sialyltransferases are viable and have very selective and often subtle phenotypes (16–28), making it difficult to predict the effect of a sialyltransferase inhibitor post-development.

Here, we show that 3F-NeuAc dramatically alters sialoside expression in mice. A single dose of 3F-NeuAc produces long lasting decreases in sialoside expression in all tissues analyzed. Decreasing sialoside expression with 3F-NeuAc results in kidney and liver dysfunction, the former of which is irreversible. These results demonstrate that global sialoside expression levels can be modulated in mice by pharmacological means and reveal that kidney and liver function are extremely sensitive to decreases in sialoside expression.

EXPERIMENTAL PROCEDURES

Animal Studies—The Scripps Research Institute Institutional Animal Care and Use Committee approved all experimental procedures involving mice. WT C57BL/6J mice were obtained from the Scripps Research Institute rodent breeding colony.

Synthesis of 2,4,7,8,9-Pentaacetyl-$3F_{ax}$-Neu5Ac-CO₂Me (3F-NeuAc)—Methyl 5-acetamido-4,7,8,9-tetra-O-acetyl-2,6-anhydro-3,5-dideoxy-D-galactonon-2-enonate (23.8 g, 50.3 mmol, 1 eq) was dissolved in nitromethane (197 ml), and H_2O (33 ml) was added. Select-Fluor (71.3 g, 201.2 mmol, 4 eq) was added, and the reaction was left to vigorously stir for 2 days at room temperature. The reaction was quenched with saturated aqueous $NaHCO_3$ (250 ml), diluted with H_2O (150 ml), and extracted three times with EtOAc (500 ml). The extracts were then further extracted with $NaHCO_3$ (300 ml), brine (300 ml), and dried over Na_2SO_4. The crude material was dissolved in EtOAc and loaded onto a silica gel column eluting with 3:7 EtOAc:Hex → 1:9 EtOAc:Hex to afford 5.12 g of 4,7,8,9-tet-

raacetyl-$3F_{eq}$-Neu5Ac-CO₂Me (compound 3), 4.74 g of a mixture of equatorial and axial diastereomers (compound 2 and 3), and 8.4 g of the desired product 4,7,8,9-tetraacetyl-$3F_{ax}$-Neu5Ac-CO₂Me (compound 2, 16.5 mmol, 33% yield). To synthesize 2,4,7,8,9-pentaacetyl-$3F_{ax}$-Neu5Ac-CO₂Me (compound 4), compound 2 (7.17 g, 14.1 mmol, 1 eq) was dissolved in pyridine (250 ml), to which acetic anhydride (3.3 ml, 35.2 mmol, 2.5 eq) was added, and the reaction was left to stir overnight. After evaporation to dryness, the residue was diluted with EtOAc (1 liter) and extracted with 5% citric acid (3×300 ml), saturated aqueous $NaHCO_3$ (300 ml), brine (300 ml), and dried over Na_2SO_4. The extracted material was then recrystallized from EtOAc/hexanes to afford the final product (5.7 g, 10.33 mmol, 73% yield). Characterization of all compounds was consistent with the previously reported data (29, 35).

Treatment of Mice with 3F-NeuAc—Male C57BL/6J mice, 6 weeks old, received 10, 30, 100, or 300 mg·kg^{-1} body weight doses of peracetylated $3F_{ax}$-NeuAc (3F-NeuAc) in 100-μl volumes delivered intravenously or intraperitoneally once daily for 1 or 7 day(s). For intravenous delivery via tail vein injection, 3F-NeuAc was dissolved in DMSO, diluted 5-fold in saline warmed to 50 °C, and vortexed immediately. For intraperitoneal delivery, 3F-NeuAc was dissolved in DMSO and diluted 2-fold in PEG300. For all studies, untreated mice received the vehicle as a control. Mice were monitored daily for signs of discomfort.

Treatment of Mice with ManNAc—N-Acetyl-D-mannosamine (ManNAc; Carbosynth) was added to the drinking water to achieve a dose of 2 g·kg^{-1}·day^{-1}. ManNAc treatment started 1 day prior to dosing with 3F-NeuAc and was not withdrawn.

Flow Cytometry Analysis—Blood (50 μl) was obtained via retro-orbital bleed. After red blood cell lysis, washed cells were stained with B220, Thy1.2, Gr1, F4/80, and lectins in Hanks' balanced salt solution containing 0.1% BSA and 2mM $CaCl_2$ for 1 h on ice. Washed cells were resuspended in the same buffer with propidium iodide prior to analysis by flow cytometry. Lectins used were FITC-*Sambucus nigra* agglutinin (SNA; Vector Laboratories, 2 μg/ml), FITC-peanut agglutinin (PNA; Vector Laboratories, 0.5 μg/ml), or human E-selectin Fc (R&D Systems, 1 μg/ml) precomplexed with goat anti-human Fcγ fragment specific IgG (Jackson ImmunoResearch, 0.5 μg/ml).

Histology and Lectin Histochemistry—Formalin-fixed paraffin embedded tissue sections (3 μm) were processed for hematoxylin and eosin staining. Carnoy's solution-fixed paraffin-embedded tissue sections were processed for lectin histochemistry. Sections were treated with 3% hydrogen peroxide in methanol for 30 min to block endogenous peroxidase and incubated in 10 mM citrate buffer, pH 6.0, for 40 min at 85 °C. Sections were blocked in Hanks' balanced salt solution containing 5% BSA and 2 mM $CaCl_2$ for 30 min and rocked overnight at 4 °C with biotinylated SNA (spleen, brain, lung, and heart, 1:3,000; liver, 1:10,000; kidney, 1:1,000), PNA (1:10,000), or *Maackia amurensis* agglutinin (MAA; 1:1,000) in blocking buffer. All biotinylated lectins were purchased from Vector Laboratories. Sections were incubated with avidin-HRP (Vectastain Elite ABC kit; Vector Laboratories) for 1 h, washed, and

developed for 10 min with peroxidase substrate (Vector Laboratories). Distilled water-washed sections were dehydrated following hematoxylin staining, and coverslips were mounted with Cytoseal (Richard Allan Scientific). Slides were scanned with a Leica SCN400 slide scanner, and images were captured using SlidePath's Digital Image Hub.

Mass Spectrometry Analysis—Sample processing for *N*- and *O*-glycomic profiling of the mouse tissues was carried out as described previously (37, 38). The tissue preparations were subjected to homogenization, reduction, carboxymethylation, and tryptic digestion. Peptide *N*-glycosidase F digestion of the purified tryptic glycopeptides was carried out in 50 mM ammonium bicarbonate, pH 8.5, for 24 h at 37 °C (Roche Applied Science). The released *N*-glycans were purified using a Sep-Pak C18 cartridge (Waters Corp.). *O*-Linked glycans were released by reductive elimination. The purified native glycans were subsequently permethylated using the sodium hydroxide procedure and purified using a Sep-Pak C18 cartridge. The permethylated glycans were then dissolved in methanol before an aliquot was mixed at a 1:1 ratio (v/v) with 10 mg/ml 3,4-diaminobenzophenone in 75% acetonitrile. The glycan matrix mixture was spotted on a stainless steel target plate and dried in a vacuum. MALDI-TOF MS data were obtained using a 4800 MALDI-TOF/TOF mass spectrometer (AB Sciex UK Limited) in the positive ion mode. The obtained MS data were viewed and processed using Data Explorer 4.9 (AB Sciex UK Limited). Manual assignment of glycan sequences was done on the basis of knowledge of mammalian biosynthetic pathways with the aid of the glycobioinformatics tool GlycoWorkBench (38) and confirmed by MS/MS.

Urine Analysis and Blood Chemistry—Urine was collected directly into a tube, while individual mice were restrained. Urine samples, pooled from a minimum of four mice per group, were boiled at 85 °C for 15 min in SDS loading buffer (Invitrogen) containing 150 mM DTT. Samples were diluted 10-fold in 1× loading buffer, resolved by SDS-PAGE (Invitrogen NuPage, 4–12%) for 75 min at 150 V, and stained with Coomassie Blue. Antech Diagnostics performed comprehensive blood chemistry on serum pooled from groups of four mice.

Western Blotting—Freshly harvested kidneys were flash frozen in liquid nitrogen and stored at −80 °C until processing. Frozen kidneys were ground to a powder with a prechilled mortar and pestle and homogenized (IKA; 30 s, power 3) in 20 volumes (by weight) of lysis solution (20 mM Tris, 150 mM NaCl, 1 mM EDTA, 1% Triton X-100, 10 mM NaF, 2 mM Na_3VO_4, pH 7.5). Lysates were cleared at $17,000 \times g$ for 10 min at 4 °C and boiled as described above for urine analysis. Lysates further diluted 10-fold in 1× SDS-PAGE loading buffer were resolved by SDS-PAGE (Invitrogen NuPage, 4–12%) for 2.5 h at 150 V and transferred to nitrocellulose membranes (30 V for 2 h). Membranes were blocked in 5% milk/TBS-T for 1 h prior to probing with anti-podocalyxin (R&D Systems, 1:2,000) in 1% BSA/TBS-T overnight at 4 °C. Blots were washed four times with TBS-T, probed with HRP-conjugated anti-goat IgG (Santa Cruz Biotechnologies, 1:20,000) for 1 h at room temperature, and developed with ECL Prime substrate (GE Healthcare) after four washes.

Immunoprecipitation of Podocalyxin—Kidneys were lysed as described for Western blotting. Lysate supernatants were diluted a further 2-fold in PBS and precleared by incubation with rProtein G-agarose (Invitrogen) at 4 °C for 1 h. Supernatants were collected and precipitated with anti-podocalyxin (R&D Systems, 1:100) overnight at 4 °C. The following day, antibodies were captured with 50 μl of rProtein G-agarose beads for 2 h at 4 °C. The precipitated complexes were washed twice with lysis buffer and twice with PBS prior to elution with 50 μl of SDS-PAGE loading buffer and immunoblotting as indicated above. Biotinylated MAA and PNA were used at a concentration of 1:5,000 along with avidin-HRP (Biolegend, 1:10,000).

RESULTS

Treatment of Mice with 3F-NeuAc Decreases Sialoside Expression on Leukocytes—To determine whether peracetylated 3F-NeuAc is active *in vivo*, we administered the compound to mice and monitored sialoside expression levels on peripheral blood leukocytes by flow cytometry. Two lectins were initially used to detect changes in sialylation: SNA, which is highly specific for the sequence NeuAcα2–6Galβ1–4GlcNAc elaborated by the sialyltransferase ST6Gal1, and PNA, which recognizes the nonsialylated sequence Galβ1–3GalNAc, which reveals blockade of the enzymatic activity of ST3Gal1, ST3Gal2, or ST3Gal3 that construct the sialylated product NeuAcα2–3Galβ1–3GalNAc. A single intravenous injection of 300 mg·kg^{-1} 3F-NeuAc produced a significant decrease in SNA staining and a concomitant increase in PNA staining on B cells (Fig. 1, *A* and *B*). Maximal effects on SNA and PNA staining of B cells were maintained for nearly 3 weeks after dosing and took ∼5 weeks to return to baseline. As an alternative dosing regimen, 3F-NeuAc was administered intraperitoneally once daily for 7 days. In this case, significant effects on SNA and PNA staining of B cells were seen down to a dose of 30 mg·kg^{-1}·day^{-1} and were sustained over 4 weeks (Fig. 1, *C* and *D*). Reductions in sialoside expression detected with SNA and PNA were also seen with T cells, but they were less pronounced (Fig. 1*E*). For granulocytes, continuous dosing at 100 mg·kg^{-1}·day^{-1} gave rise to an increase in PNA staining and a decrease in E-selectin staining, which recognizes the terminal sequence sialyl-Lewis^X (NeuAcα2–3Galβ1–4(α1–3Fuc)GlcNAc) (Fig. 1*F*). These results demonstrate that 3F-NeuAc effectively decreases cell surface sialylation on peripheral leukocytes *in vivo*, with different cell types exhibiting differential sensitivity.

Treatment of Mice with 3F-NeuAc Alters Sialoside Expression in Numerous Tissues—Lectin histochemical studies were performed on day 11 paraffin-embedded tissue sections from mice treated with a single dose of 300 mg·kg^{-1} (Fig. 2). Most tissues, including the spleen, liver, brain, and kidney, revealed decreased SNA and increased PNA staining relative to tissues from untreated mice (Fig. 2, *A–C* and *F*). Lung and heart tissues also showed increased PNA staining (Fig. 2, *D* and *E*). In all tissues, changes in staining intensity were not uniform, reflecting the differential expression of the affected sialyltransferases and/or sensitivity to the inhibitor as seen by flow cytometry with leukocytes. In some tissues such as the spleen, brain, and kidney, changes in SNA and PNA staining were particularly localized to specialized substructures in these organs. For
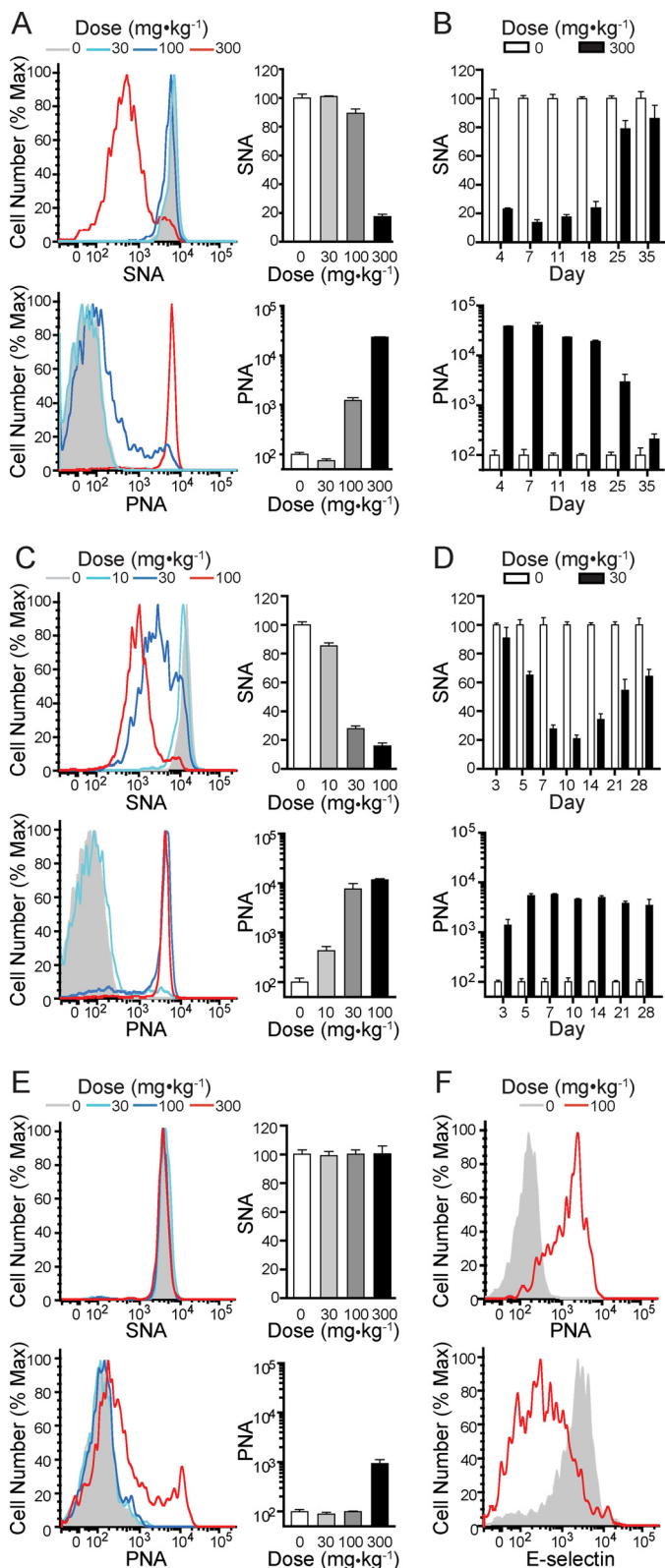
FIGURE 1. **Administration of 3F-NeuAc to mice results in dose- and time-dependent decreases in sialoside expression on peripheral blood leukocytes.** *A*, SNA (*upper panels*) and PNA (*lower panels*) staining on B cells 11 days after mice received one of the indicated single intravenous doses of 3F-NeuAc. *B*, time course summary of SNA (*upper panels*) and PNA (*lower panels*) staining on B cells from mice that received a single 300 mg·kg^{-1} intravenous injection of 3F-NeuAc. *C*, SNA (*upper*) and PNA (*lower*) staining on B cells (day 11) from mice that received a daily intraperitoneal injection of 3F-NeuAc at one of the indicated doses for 7 days. *D*, time course summary of SNA (*upper*)
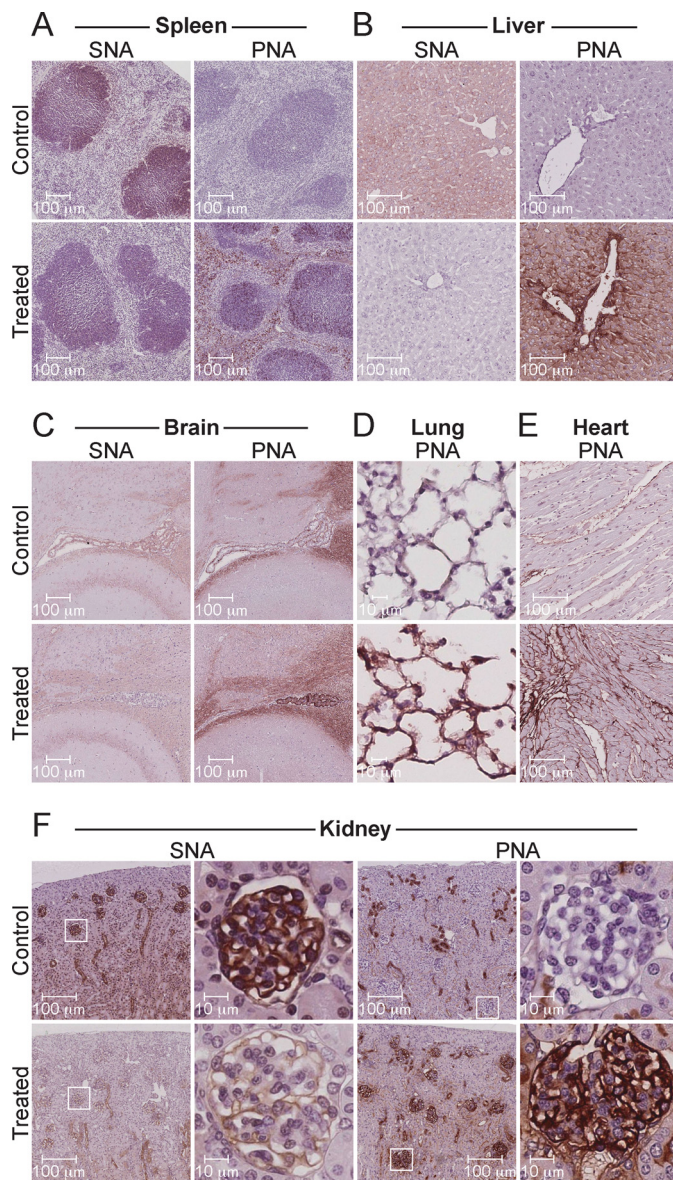

FIGURE 2. **Administration of 3F-NeuAc to mice abrogates sialoside expression in key tissues.** Lectin histochemical staining of spleen (*A*), liver (*B*), brain (*C*), lung (*D*), heart (*E*), and kidney (*F*) sections from mice treated once with 300 mg·kg^{-1} of 3F-NeuAc or vehicle. Tissues from treated mice display marked changes in SNA and PNA staining; however, the most obvious changes can be seen in the kidney glomeruli (*F*, high magnification). All tissues were harvested 11 days after treatment, fixed, paraffin-embedded, stained with the indicated biotinylated lectin, developed with avidin-HRP and Vector NovaRED, and counterstained with hematoxylin. The images are representative of two mice for each condition.

example, in the spleen of treated mice, cells within regions of high cellularity, consistent with the B cell follicle, show significant changes in SNA and PNA staining (Fig. 2*A*). In the brain, the most apparent differences are observed in the choroid

and PNA (*lower*) staining on B cells from mice that received a daily 30 mg·kg^{-1} intraperitoneal injection of 3F-NeuAc for 7 days. *E*, SNA (*upper*) and PNA (*lower*) staining on T cells 11 days after mice received one of the indicated single intravenous doses of 3F-NeuAc. *F*, PNA (*upper*) and E-selectin (*lower*) staining on granulocytes (day 7) from mice that received a daily intraperitoneal injection of 100 mg·kg^{-1}·day^{-1} 3F-NeuAc for 7 days. All data represent the means ± S.E. of four replicates, are expressed as percentages relative to mice that received vehicle, and are representative of three independent experiments. *Max*, maximum.
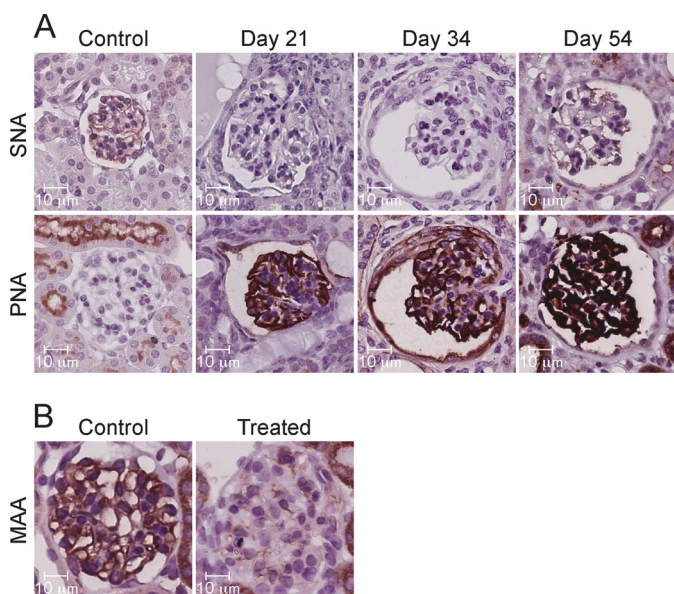
FIGURE 3. Administration of 3F-NeuAc to mice results in long lasting altered sialoside expression in glomeruli. Histochemical staining of paraffin-embedded kidney sections with biotinylated lectins SNA and PNA (*A*) and MAA (*B*) shows distinct changes in the glomeruli after mice received a single 300 mg·kg^{-1} intravenous dose of 3F-NeuAc. Tissues stained with MAA were harvested 11 days after treatment. All tissues were counterstained with hematoxylin. The data are representative of two mice and a minimum of 30 glomeruli from each.

plexus of the hippocampus (Fig. 2C). The kidneys of treated mice display decreased sialoside expression that is most prominent in the glomeruli (Fig. 2F, high magnification). The altered SNA and PNA staining was long lasting, with glomeruli still displaying changes 54 days after treatment with a single 300 mg·kg^{-1} dose of 3F-NeuAc (Fig. 3A). Furthermore, staining by MAA, which predominantly recognizes $\alpha2-3$ sialosides, was reduced in treated tissues (Fig. 3B). These results show that 3F-NeuAc is effective in decreasing sialoside expression throughout many tissues for an extended period of time.

MS Glycan Profiling Reveals Altered Sialoside Expression in 3F-NeuAc-treated Mice—To further address the effects of 3F-NeuAc on glycan expression in greater molecular detail, mass spectrometry of permethylated glycans was carried out on liver, spleen, kidney, and testes 11 days after treatment of mice with a single 300 mg·kg^{-1} dose of 3F-NeuAc or control vehicle. Profound differences were observed in the liver (Fig. 4A and supplemental Fig. S1), where there was a dramatic decrease in the abundance of sialylated N-glycans. As shown for the low molecular weight portion of the spectrum in Fig. 4A, sialylated glycans with NeuGc, a murine sialic acid with an N-glycolyl group (1), were absent or reduced in the treated tissue and replaced by the appearance of nonsialylated species capped with galactose or additional LacNAc (Gal-GlcNAc) repeats. Longer LacNAc repeats, which were also observed previously in cultured cells treated with 3F-NeuAc (29), are likely a consequence of glycans not being "capped" by the sialyltransferases, which compete with the $\beta1,3$-N-acetylglucosaminyl and $\beta1,4$ galactosyltransferases that add additional LacNAc repeats. This was also evident for higher molecular weight glycans from the liver where NeuGc capped with di-, tri-, and tetra-antennary N-glycans was decreased or missing in 3F-NeuAc-treated mice,

and neutral glycans were increased in vehicle-treated mice. This dramatic change is consistent with the uniform changes in lectin staining in the liver (Fig. 2B) and likely reflects the changes in hepatocytes, which are the predominate cell type.

Significant reductions in sialylated N-linked glycans were also seen in the spleen (Fig. 4B and supplemental Fig. S2) and testes (supplemental Fig. S3) of treated mice. Several sialylated glycans showed major changes in the spleen, whereas others were less affected. This likely reflects the fact that the spleen is predominantly a mixture of B and T cells, which showed different sensitivity to 3F-NeuAc as judged from flow cytometry with SNA and PNA (Fig. 1).

In contrast, the glycan profiles from kidneys of treated mice displayed more subtle differences. Unlike the glycomes of other organs, the majority of kidney N-linked glycans are terminated by fucose instead of sialic acid (39, 40); therefore, it is not surprising that the most abundant N-linked glycans (supplemental Fig. S4, A–H) were retained at high levels in the treated mice. Although in low abundance, several sialylated glycans were dramatically reduced, including a di-NeuGc biantennary glycan (*m/z* 2852), although other sialylated glycans were less affected. Reductions in sialylated glycans were accompanied by an increase in galactose-terminated glycans, including the appearance of a major nonsialylated biantennary glycan at *m/z* 2070. The O-linked glycans (supplemental Fig. S4, I and J) also showed reductions in NeuGc-containing glycans, whereas NeuAc levels were only modestly affected. The reduction in the overall O-sialoglycome was accompanied by a corresponding increase in the level of the T antigen, Gal$\beta1-3$GalNAc, consistent with the increased PNA staining of treated tissue, which recognizes this sequence as a ligand (Fig. 2F). Taken together, the glycan profile analysis provides further direct evidence for the impact of 3F-NeuAc on sialoside expression of many cells and tissues and is consistent with the observation that certain cells and glycan structures are more affected than others.

A Single Dose of 3F-NeuAc Causes Mice to Develop Kidney and Liver Dysfunction—In the course of our studies, we noticed that treatment with 3F-NeuAc resulted in weight fluctuation in the mice. A large group of mice treated with a single 300 mg·kg^{-1} dose of 3F-NeuAc displayed a reproducible phase of rapid weight gain, starting 7 days after treatment (Fig. 5A), which occurred concomitantly with systemic edema in the peritoneal cavity. Weight gain was followed shortly thereafter by substantial weight loss, and all mice given a single 300 mg·kg^{-1} dose of 3F-NeuAc died or reached the study end point (20% body weight loss) by day 54 (Fig. 5B). Mice treated with a 100 mg·kg^{-1} dose of 3F-NeuAc daily for 7 days had even more pronounced weight loss and died by day 15 (data not shown). Interestingly, daily co-administration of 2 g·kg^{-1} ManNAc in the drinking water, a sialic acid precursor, which should increase the levels of CMP-NeuAc, did not prevent the effects of a single 300 mg·kg^{-1} dose of 3F-NeuAc (Fig. 6).

Because edema can be caused by loss of protein from the blood caused by kidney dysfunction (41), we analyzed the blood and urine of treated mice and, indeed, found that 300 mg·kg^{-1} of 3F-NeuAc decreased total protein and albumin in the blood (Table 1) and resulted in large amounts of albumin in the urine (Fig. 5C). A single dose lower than 300 mg·kg^{-1} did not result in
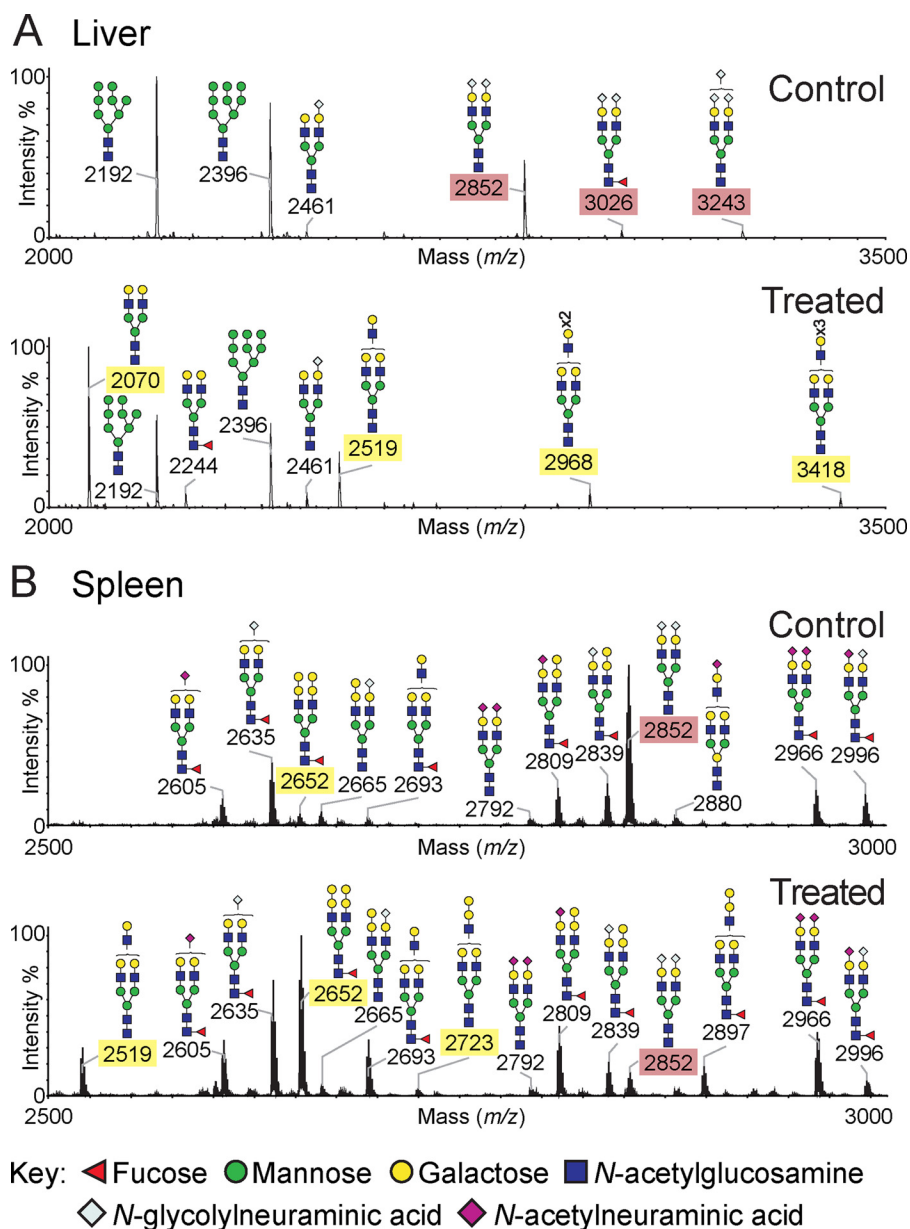
≋ASBMB

FIGURE 4. **MS glycan profiling of tissues from 3F-NeuAc-treated mice reveals altered sialosides.** *N*-Glycans from liver (*A*) and spleen (*B*) were released by peptide *N*-glycosidase F and permethylated. The data were acquired in the positive ion mode to observe $[M + Na]^+$ molecular ions. Structures shown outside a *bracket* have not had their antenna location unequivocally defined. For clarity, the sialylated and desialylated glycan species that differ between the control tissues and those taken from mice 11 days after a single injection of 300 mg·kg^{-1} 3F-NeuAc have been highlighted with *red* and *yellow rectangles*, respectively. The data are representative of three replicates for each condition.

altered urinary protein levels (Fig. 5*D*) or levels of serum albumin, blood urea nitrogen, phosphorus, and cholesterol (Table 1). The kidneys of treated mice were analyzed in further detail by hematoxylin and eosin staining, which revealed gross histological changes beginning with tubular protein casts by day 11 and severely distorted and sclerosed glomeruli by day 21 (Fig. 5*E*). Moreover, we observed loss of sialylation of podocalyxin, a protein expressed in the secondary foot processes of podocytes within the glomerulus, in immunoblots of whole kidney lysates from treated mice. As shown in Fig. 5*F*, we noted a remarkable change in the electrophoretic mobility, consistent with a loss of negatively charged sialic acid, of this glycoprotein. In addition, we found that immunoprecipitated protein had decreased

MAA staining by Western blot, and a concomitant increase in PNA staining (Fig. 5*G*).

In addition to the above noted kidney dysfunction, we were also able to detect changes in blood chemistry in mice treated with 3F-NeuAc that are consistent with liver dysfunction. Severely altered liver enzymes (aspartate aminotransferase (AST), alanine aminotransferase (ALT), and alkaline phosphatase (ALP)) were detected in mice treated with 300 mg·kg^{-1} of 3F-NeuAc, and even modest changes were detected at a dose of 100 mg·kg^{-1} (Table 1). The fact that kidney dysfunction is not noted at this lower dose suggests that liver dysfunction is not a secondary consequence of kidney dysfunction. Nevertheless, histological analysis of the liver from treated mice did not reveal
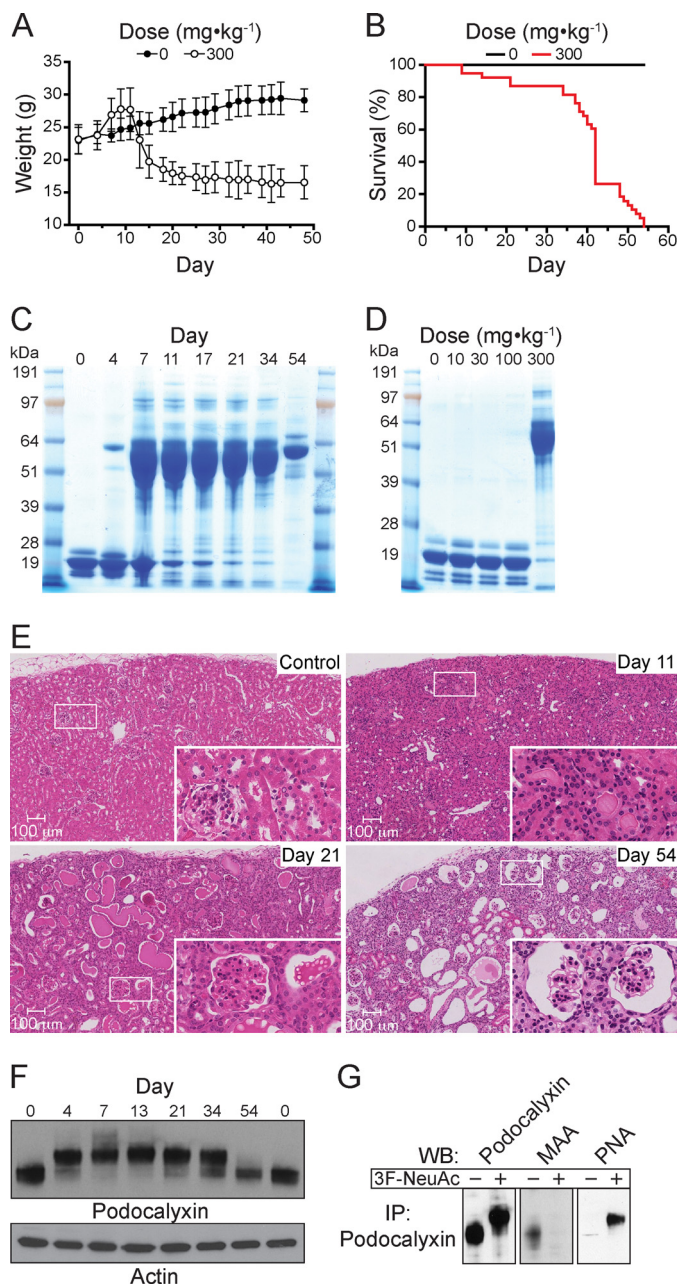
FIGURE 5. **Decreased sialoside expression in the kidney results in dysfunction, proteinuria, and lethality.** *A*, average body weight of mice (*n* = 44 to start the experiment) treated with a single intravenous injection of 300 mg·kg^{-1} 3F-NeuAc reveals a phase of weight gain followed by substantial weight loss. The data represent the means ± S.E. and are representative of three independent experiments. *B*, survival curve of mice (*n* = 44) treated with a single intravenous injection of 300 mg·kg^{-1} 3F-NeuAc demonstrates that all mice died or reached the study end point by day 54. The data are representative of three independent experiments. *C*, SDS-PAGE analysis of urine over the course of 54 days from mice treated with a single intravenous injection of 300 mg·kg^{-1} 3F-NeuAc reveals proteinuria, demonstrated by the excretion of large quantities of albumin into the urine. *D*, SDS-PAGE analysis of urine pooled from mice that received one of the indicated single doses of 3F-NeuAc, ranging from 10 to 300 mg·kg^{-1}. *E*, hematoxylin and eosin staining shows gross histological changes in the kidney beginning 11 days after a single injection of 3F-NeuAc, tubular protein casts by day 21, and severely distorted glomerular and tubular architecture by day 54. *F*, immunoblots of whole kidney lysates for podocalyxin on the indicated days following treatment with 3F-NeuAc show the desialylation of podocalyxin and subsequent re-sialylation by day 54. *G*, immunoprecipitation (*IP*) of podocalyxin and subsequent Western blotting (*WB*) with the lectins MAA and PNA demonstrate that podocalyxin sialylation is abrogated in mice treated with 3F-NeuAc.
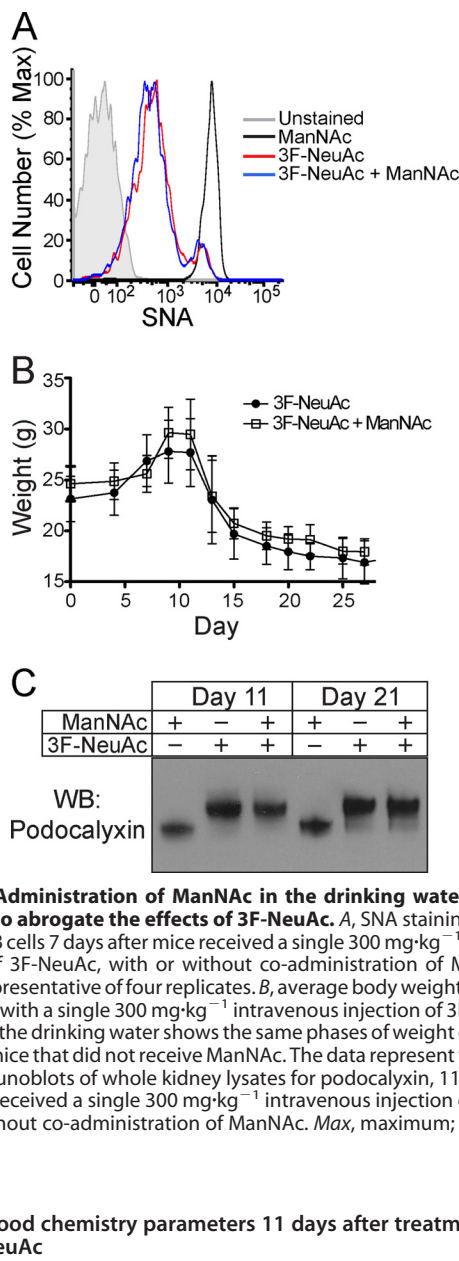

FIGURE 6. **Administration of ManNAc in the drinking water of treated mice fails to abrogate the effects of 3F-NeuAc.** *A*, SNA staining on peripheral blood B cells 7 days after mice received a single 300 mg·kg^{-1} intravenous injection of 3F-NeuAc, with or without co-administration of ManNAc. The data are representative of four replicates. *B*, average body weight of mice (*n* = 16) treated with a single 300 mg·kg^{-1} intravenous injection of 3F-NeuAc and ManNAc in the drinking water shows the same phases of weight gain and loss as seen in mice that did not receive ManNAc. The data represent the means ± S.E. *C*, immunoblots of whole kidney lysates for podocalyxin, 11 and 21 days after mice received a single 300 mg·kg^{-1} intravenous injection of 3F-NeuAc, with or without co-administration of ManNAc. *Max*, maximum; *WB*, Western blotting.

TABLE 1

Altered blood chemistry parameters 11 days after treatment of mice with 3F-NeuAc

AST, aspartate aminotransferase; ALT, alanine aminotransferase; ALP, alkaline phosphatase; BUN, blood urea nitrogen.

Parameter	Results			
	0 mg·kg^{-1}	30 mg·kg^{-1}	100 mg·kg^{-1}	300 mg·kg^{-1}
Total protein (g/dl)	5.0	5.1	5.1	3.2
Albumin (g/dl)	2.6	2.7	2.8	1.2
AST (IU/liter)	59	67	95	151
ALT (IU/liter)	62	54	83	140
ALP (IU/liter)	104	155	820	1276
BUN (mg/dl)	22	24	23	97
Phosphorus (mg/dl)	6.0	5.8	7.3	10.6
Cholesterol (mg/dl)	122	136	152	315

any gross abnormalities (data not shown). Taken together, the massive physiological perturbations induced by 3F-NeuAc underscore the vital roles played by sialic acid in adult mice.

DISCUSSION

We have shown herein that *in vivo* administration of 3F-NeuAc systemically decreases sialosides in various mouse

In Vivo Use of a Global Sialyltransferase Inhibitor

cells and tissues. We noted several examples of differential sensitivity of cell types to 3F-NeuAc. In the blood, flow cytometry analysis with sialic acid-sensitive lectins showed that sialoside expression on B cells was dramatically decreased by treatment with 3F-NeuAc, whereas the corresponding changes on T cells and neutrophils were minimal. Similarly, immunohistochemical staining revealed that glomeruli in the kidney were highly sensitive to 3F-NeuAc and had altered sialoside expression for over 50 days, whereas less dramatic changes were seen in the parenchyma. Several reasons may account for such differences. Because the inhibitor will only prevent sialylation of newly synthesized proteins, an impact on sialylation will be most evident with metabolically active tissues with high turnover of membrane proteins. Thus, it is perhaps not surprising that liver showed dramatic changes in sialylated glycans by MS glycomics profiling. Other factors may contribute such as uptake of the inhibitor, ability of cells to convert 3F-NeuAc into CMP-3F-NeuAc, endogenous levels of CMP-NeuAc, and differential sensitivity of individual sialyltransferases to CMP-3F-NeuAc inhibition, as well as the unique expression patterns of sialyltransferases in different cell types (29, 39). Regardless, long lasting changes in sialoside levels were evident in all tissues tested from mice treated with 3F-NeuAc.

Although all organs analyzed showed losses in cellular sialylation, profound kidney dysfunction was the most prominent phenotype we observed in mice treated with 3F-NeuAc. With only a single dose of 3F-NeuAc (300 mg·kg^{-1}), mice acquired characteristics of nephritic syndrome, where glomerular filtration is compromised, resulting in edema, excretion of albumin in the urine, and loss of protein from the blood (41). Dramatic changes in sialoside expression were observed in the glomeruli and a subset of tubules, leading to glomerulosclerosis at later time points and the appearance of precipitated protein within the lumen of the tubules. These changes are likely a reflection of the loss of sialic acid on podocalyxin, a highly sialylated glycoprotein on glomerular podocytes that forms an electrostatic barrier integral to the filtering capacity of glomeruli (42). Indeed, loss of sialylation on podocalyxin is known to cause kidney dysfunction in patients as well as mice with mutations in glucosamine [UDP-N-acetyl]-2-epimerase/N-acetylmannosamine kinase and cytidine monophosphate N-acetylneuraminic acid synthetase (32–34). The resialylation of podocalyxin by day 54 as seen by Western blot but continued loss of kidney function may reflect the desialylation on other highly sialylated proteins, such as nephrin, which also serves a critical filtration role in podocytes (34). To this end, the dramatic loss of sialic acid on podocalyxin that we observed after treatment of mice with 3F-NeuAc strongly correlated with kidney dysfunction and the onset of proteinuria. This "on target" effect of 3FNeuAc confirms the critical role of sialylation of podocalyxin for its function in glomerular filtration in adult mice.

Deleterious effects on the liver, as manifested by abnormal levels of liver enzymes in the blood, were seen after a single 100 mg·kg^{-1} dose of 3F-NeuAc, when no effects on the kidneys were observed. Altered liver enzymes were found in several sialyltransferase-deficient mice (19). We suggest that high levels of serum glycoproteins containing unmasked galactose residues that will be exposed without terminal sialylation may overwhelm the hepatocyte asialoglycoprotein receptor that normally clears these proteins, and the resulting stress may alter liver function.

In our original study describing 3F-NeuAc, we demonstrated that it is converted into CMP-3F-NeuAc within the cell, where it accumulates to high levels (29). Although CMP-3F-NeuAc is a direct inhibitor of sialyltransferases (30, 31), it can also cause depletion of CMP-NeuAc as a result of feedback inhibition of the sialic acid biosynthetic pathway, which by itself could account for loss in synthesis of sialoglycoproteins (29). To test the importance of substrate depletion, we co-administered ManNAc, a sialic acid precursor that enters the sialic acid biosynthetic pathway downstream of the step that is feedback inhibited by CMP-3F-NeuAc. We found that ManNAc, administered to mice at a dose exceeding that previously used to rescue genetic mutations in glucosamine [UDP-N-acetyl]-2-epimerase/N-acetylmannosamine kinase (32), failed to abrogate any of the effects of 3F-NeuAc. A recent study also showed that ManNAc failed to rescue the ability of 3F-NeuAc to decrease sialoside expression in cultured cells (43). Thus, direct inhibition of sialyltransferases by the accumulated CMP-3F-NeuAc appears to be sufficient to cause the observed decreases in sialylation.

There is now a growing class of sugar analogs that modulate cellular glycosylation by a mechanism that involves their intracellular conversion to nucleotide sugars, which are recognized as donor substrates for the corresponding glycosyltransferases but are poorly transferred, effectively making them inhibitors (29, 44–47). In our original report describing 3F-NeuAc, we showed that 2F-Fuc was similarly converted by cells to GDP-2F-Fuc and blocked cellular fucosyltransferases (29). This analog was discovered independently by another group and shown to block fucosylation in mice (47). Unlike with 3F-NeuAc, the effects of 2F-Fuc are completely reversible within a few days. Furthermore, mice treated with high doses of 2F-Fuc were reported as being healthy (47), suggesting that global blockade of fucosylation is more tolerated than blockade of sialylation. Another fluoro-sugar, 4F-GlcNAc, has been demonstrated to impact terminal glycosylation of leukocytes *in vivo* (46). Because it diminishes levels of endogenous UDP-GlcNAc in cells, but it is not transferred to glycoproteins (46), its mechanism of action likely involves inhibition of N-acetylglucosamine transferases by UDP-4F-GlcNAc. The first sugar analog documented as a metabolic inhibitor of glycosyltransferases was 5S-GlcNAc, which is converted by cells to the corresponding UDP-5S-GlcNAc. Interestingly, its impact on glycosylation was most dramatic on products of the cytosolic O-GlcNAc transferase (44). The related 5S-Fuc was also shown to be converted to GDP-5S-Fuc and inhibit fucosyltransferases similar to 2F-Fuc (45). Although thio-sugars have not been evaluated *in vivo*, the collective data suggest that both fluoro- and thio-sugar analogs will prove to be useful tools for investigating the *in vivo* roles of glycosylation.

In summary, inhibiting sialyltransferases is an attractive strategy to investigate the biological roles of sialic acid and potentially treat diseases involving sialic acid recognition, such as autoimmunity (16), cancer metastasis (11), and influenza (36). Although the use of 3F-NeuAc *in vivo* has some limita-

tions, predominantly because of renal failure, the prolonged effect of 3F-NeuAc can be exploited for *in vivo* experiments, as shown recently by decreased adhesion and migration of cancer cells after *in vitro* treatment with 3F-NeuAc to block sialylation (43). Our demonstration that 3F-NeuAc causes systemic blockade of sialylation *in vivo* documents the potential for more selective sialyltransferase inhibitors. Because mice deficient in individual sialyltransferases have relatively mild phenotypes and no reported kidney dysfunction (16–28), the time is ripe for the development of selective, small molecule inhibitors of these enzymes to study the biological roles of sialylated glycans and decrease sialoside expression for therapeutic use.

REFERENCES

1. Angata, T., and Varki, A. (2002) Chemical diversity in the sialic acids and related α-keto acids: an evolutionary perspective. *Chem. Rev.* **102,** 439–469
2. Varki, A. (2007) Glycan-based interactions involving vertebrate sialic-acid-recognizing proteins. *Nature* **446,** 1023–1029
3. Rosen, S. D. (2004) Ligands for L-selectin: homing, inflammation, and beyond. *Annu. Rev. Immunol.* **22,** 129–156
4. Crocker, P. R., Paulson, J. C., and Varki, A. (2007) Siglecs and their roles in the immune system. *Nat. Rev. Immunol.* **7,** 255–266
5. Neu, U., Bauer, J., and Stehle, T. (2011) Viruses and sialic acids: rules of engagement. *Curr. Opin. Struct. Biol.* **21,** 610–618
6. Pang, P. C., Chiu, P. C., Lee, C. L., Chang, L. Y., Panico, M., Morris, H. R., Haslam, S. M., Khoo, K. H., Clark, G. F., Yeung, W. S., and Dell, A. (2011) Human sperm binding is mediated by the sialyl-Lewis(x) oligosaccharide on the zona pellucida. *Science* **333,** 1761–1764
7. Hildebrandt, H., and Dityatev, A. (2013) Polysialic acid in brain development and synaptic plasticity. *Top. Curr. Chem.*, in press
8. Ednie, A. R., and Bennett, E. S. (2012) Modulation of voltage-gated ion channels by sialylation. *Compr. Physiol.* **2,** 1269–1301
9. Quaggin, S. E. (2007) Sizing up sialic acid in glomerular disease. *J. Clin. Invest.* **117,** 1480–1483
10. Schwarzkopf, M., Knobeloch, K.-P., Rohde, E., Hinderlich, S., Wiechens, N., Lucka, L., Horak, I., Reutter, W., and Horstkorte, R. (2002) Sialylation is essential for early development in mice. *Proc. Natl. Acad. Sci. U.S.A.* **99,** 5267–5270
11. Fuster, M. M., and Esko, J. D. (2005) The sweet and sour of cancer: glycans as novel therapeutic targets. *Nat. Rev. Cancer* **5,** 526–542
12. Paulson, J. C., and Rademacher, C. (2009) Glycan terminator. *Nat. Struct. Mol. Biol.* **16,** 1121–1122
13. Paulson, J. C., Weinstein, J., and Schauer, A. (1989) Tissue-specific expression of sialyltransferases. *J. Biol. Chem.* **264,** 10931–10934
14. Kitagawa, H., and Paulson, J. C. (1994) Differential expression of five sialyltransferase genes in human tissues. *J. Biol. Chem.* **269,** 17872–17878
15. Kono, M., Ohyama, Y., Lee, Y. C., Hamamoto, T., Kojima, N., and Tsuji, S. (1997) Mouse β-galactoside α2,3-sialyltransferases: comparison of in vitro substrate specificities and tissue specific expression. *Glycobiology* **7,** 469–479
16. Hennet, T., Chui, D., Paulson, J. C., and Marth, J. D. (1998) Immune regulation by the ST6Gal sialyltransferase. *Proc. Natl. Acad. Sci. U.S.A.* **95,** 4504–4509
17. Frommhold, D., Ludwig, A., Bixel, M. G., Zarbock, A., Babushkina, I., Weissinger, M., Cauwenberghs, S., Ellies, L. G., Marth, J. D., Beck-Sickinger, A. G., Sixt, M., Lange-Sperandio, B., Zernecke, A., Brandt, E., Weber, C., Vestweber, D., Ley, K., and Sperandio, M. (2008) Sialyltransferase ST3Gal-IV controls CXCR2-mediated firm leukocyte arrest during inflammation. *J. Exp. Med.* **205,** 1435–1446
18. Priatel, J. J., Chui, D., Hiraoka, N., Simmons, C. J., Richardson, K. B., Page, D. M., Fukuda, M., Varki, N. M., and Marth, J. D. (2000) The ST3Gal-I sialyltransferase controls CD8+ T lymphocyte homeostasis by modulating O-glycan biosynthesis. *Immunity* **12,** 273–283
19. Orr, S. L., Le, D., Long, J. M., Sobieszczuk, P., Ma, B., Tian, H., Fang, X., Paulson, J. C., Marth, J. D., and Varki, N. (2013) A phenotype survey of 36 mutant mouse strains with gene-targeted defects in glycosyltransferases or glycan-binding proteins. *Glycobiology* **23,** 363–380
20. Yang, W. H., Nussbaum, C., Grewal, P. K., Marth, J. D., and Sperandio, M. (2012) Coordinated roles of ST3Gal-VI and ST3Gal-IV sialyltransferases in the synthesis of selectin ligands. *Blood* **120,** 1015–1026
21. Ellies, L. G., Sperandio, M., Underhill, G. H., Yousif, J., Smith, M., Priatel, J. J., Kansas, G. S., Ley, K., and Marth, J. D. (2002) Sialyltransferase specificity in selectin ligand formation. *Blood* **100,** 3618–3625
22. Nagafuku, M., Okuyama, K., Onimaru, Y., Suzuki, A., Odagiri, Y., Yamashita, T., Iwasaki, K., Fujiwara, M., Takayanagi, M., Ohno, I., and Inokuchi, J. (2012) CD4 and CD8 T cells require different membrane gangliosides for activation. *Proc. Natl. Acad. Sci. U.S.A.* **109,** E336–E342
23. Eckhardt, M., Bukalo, O., Chazal, G., Wang, L., Goridis, C., Schachner, M., Gerardy-Schahn, R., Cremer, H., and Dityatev, A. (2000) Mice deficient in the polysialyltransferase ST8SiaIV/PST-1 allow discrimination of the roles of neural cell adhesion molecule protein and polysialic acid in neural development and synaptic plasticity. *J. Neurosci.* **20,** 5234–5244
24. Angata, K., Long, J. M., Bukalo, O., Lee, W., Dityatev, A., Wynshaw-Boris, A., Schachner, M., Fukuda, M., and Marth, J. D. (2004) Sialyltransferase ST8Sia-II assembles a subset of polysialic acid that directs hippocampal axonal targeting and promotes fear behavior. *J. Biol. Chem.* **279,** 32603–32613
25. Krocher, T., Malinovskaja, K., Jurgenson, M., Aonurm-Helm, A., Zharkovskaya, T., Kalda, A., Rockle, I., Schiff, M., Weinhold, B., Gerardy-Schahn, R., Hildebrandt, H., and Zharkovsky, A. (2013) Schizophrenia-like phenotype of polysialyltransferase ST8SIA2-deficient mice. *Brain Struct. Funct.*, in press
26. Yoshikawa, M., Go, S., Takasaki, K., Kakazu, Y., Ohashi, M., Nagafuku, M., Kabayama, K., Sekimoto, J., Suzuki, S., Takaiwa, K., Kimitsuki, T., Matsumoto, N., Komune, S., Kamei, D., Saito, M., Fujiwara, M., Iwasaki, K., and Inokuchi, J. (2009) Mice lacking ganglioside GM3 synthase exhibit complete hearing loss due to selective degeneration of the organ of Corti. *Proc. Natl. Acad. Sci. U.S.A.* **106,** 9483–9488
27. Okada, M., Itoh Mi, M., Haraguchi, M., Okajima, T., Inoue, M., Oishi, H., Matsuda, Y., Iwamoto, T., Kawano, T., Fukumoto, S., Miyazaki, H., Furukawa, K., and Aizawa, S. (2002) B-series Ganglioside deficiency exhibits no definite changes in the neurogenesis and the sensitivity to Fas-mediated apoptosis but impairs regeneration of the lesioned hypoglossal nerve. *J. Biol. Chem.* **277,** 1633–1636
28. Ellies, L. G., Ditto, D., Levy, G. G., Wahrenbrock, M., Ginsburg, D., Varki, A., Le, D. T., and Marth, J. D. (2002) Sialyltransferase ST3Gal-IV operates as a dominant modifier of hemostasis by concealing asialoglycoprotein receptor ligands. *Proc. Natl. Acad. Sci. U.S.A.* **99,** 10042–10047
29. Rillahan, C. D., Antonopoulos, A., Lefort, C. T., Sonon, R., Azadi, P., Ley, K., Dell, A., Haslam, S. M., and Paulson, J. C. (2012) Global metabolic inhibitors of sialyl- and fucosyltransferases remodel the glycome. *Nat. Chem. Biol.* **8,** 661–668
30. Burkart, M. D., Vincent, S. P., Düffels, A., Murray, B. W., Ley, S. V., and Wong, C. H. (2000) Chemo-enzymatic synthesis of fluorinated sugar nucleotide: useful mechanistic probes for glycosyltransferases. *Bioorg. Med. Chem.* **8,** 1937–1946
31. Lairson, L. L., Henrissat, B., Davies, G. J., and Withers, S. G. (2008) Glycosyltransferases: structures, functions, and mechanisms. *Annu. Rev. Biochem.* **77,** 521–555
32. Galeano, B., Klootwijk, R., Manoli, I., Sun, M., Ciccone, C., Darvish, D., Starost, M. F., Zerfas, P. M., Hoffmann, V. J., Hoogstraten-Miller, S., Krasnewich, D. M., Gahl, W. A., and Huizing, M. (2007) Mutation in the key enzyme of sialic acid biosynthesis causes severe glomerular proteinuria and is rescued by *N*-acetylmannosamine. *J. Clin. Invest.* **117,** 1585–1594
33. Ito, M., Sugihara, K., Asaka, T., Toyama, T., Yoshihara, T., Furuichi, K., Wada, T., and Asano, M. (2012) Glycoprotein hyposialylation gives rise to a nephrotic-like syndrome that is prevented by sialic acid administration in GNE V572L point-mutant mice. *PLoS One* **7,** e29873
34. Weinhold, B., Sellmeier, M., Schaper, W., Blume, L., Philippens, B., Kats, E., Bernard, U., Galuska, S. P., Geyer, H., Geyer, R., Worthmann, K., Schiffer, M., Groos, S., Gerardy-Schahn, R., and Münster-Kühnel, A. K. (2012) Deficits in sialylation impair podocyte maturation. *J. Am. Soc. Nephrol.* **23,** 1319–1328

35. Burkart, M., Zhang, Z., Hung, S., and Wong, C. (1997) A new method for the synthesis of fluoro-carbohydrates and glycosides using selectfluor. *J. Am. Chem. Soc.* **119,** 11743–11746

36. Nicholls, J. M., Moss, R. B., and Haslam, S. M. (2013) The use of sialidase therapy for respiratory viral infections. *Antivir. Res.* **98,** 401–409

37. North, S. J., Jang-Lee, J., Harrison, R., Canis, K., Ismail, M. N., Trollope, A., Antonopoulos, A., Pang, P. C., Grassi, P., Al-Chalabi, S., Etienne, A. T., Dell, A., and Haslam, S. M. (2010) Mass spectrometric analysis of mutant mice. *Methods Enzymol.* **478,** 27–77

38. Ceroni, A., Maass, K., Geyer, H., Geyer, R., Dell, A., and Haslam, S. M. (2008) GlycoWorkbench: a tool for the computer-assisted annotation of mass spectra of glycans. *J. Proteome Res.* **7,** 1650–1659

39. Comelli, E. M., Head, S. R., Gilmartin, T., Whisenant, T., Haslam, S. M., North, S. J., Wong, N. K., Kudo, T., Narimatsu, H., Esko, J. D., Drickamer, K., Dell, A., and Paulson, J. C. (2006) A focused microarray approach to functional glycomics: transcriptional regulation of the glycome. *Glycobiology* **16,** 117–131

40. Takamatsu, S., Antonopoulos, A., Ohtsubo, K., Ditto, D., Chiba, Y., Le, D. T., Morris, H. R., Haslam, S. M., Dell, A., Marth, J. D., and Taniguchi, N. (2010) Physiological and glycomic characterization of *N*-acetylglucosaminyltransferase-IVa and -IVb double deficient mice. *Glycobiology* **20,** 485–497

41. Orth, S. R., and Ritz, E. (1998) The nephrotic syndrome. *N. Engl. J. Med.* **338,** 1202–1211

42. Gelberg, H., Healy, L., Whiteley, H., Miller, L. A., and Vimr, E. (1996) *In vivo* enzymatic removal of $\alpha 2 \rightarrow 6$-linked sialic acid from the glomerular filtration barrier results in podocyte charge alteration and glomerular injury. *Lab. Invest.* **74,** 907–920

43. Büll, C., Boltje, T. J., Wassink, M., de Graaf, A. M., van Delft, F. L., den Brok, M. H., and Adema, G. J. (2013) Targeting aberrant sialylation in cancer cells using a fluorinated sialic acid analog impairs adhesion, migration, and in vivo tumor growth. *Mol. Cancer Ther.* **12,** 1935–1946

44. Gloster, T. M., Zandberg, W. F., Heinonen, J. E., Shen, D. L., Deng, L., and Vocadlo, D. J. (2011) Hijacking a biosynthetic pathway yields a glycosyltransferase inhibitor within cells. *Nat. Chem. Biol.* **7,** 174–181

45. Zandberg, W. F., Kumarasamy, J., Pinto, B. M., and Vocadlo, D. J. (2012) Metabolic inhibition of sialyl-Lewis X biosynthesis by 5-thiofucose remodels the cell surface and impairs selectin-mediated cell adhesion. *J. Biol. Chem.* **287,** 40021–40030

46. Barthel, S. R., Antonopoulos, A., Cedeno-Laurent, F., Schaffer, L., Hernandez, G., Patil, S. A., North, S. J., Dell, A., Matta, K. L., Neelamegham, S., Haslam, S. M., and Dimitroff, C. J. (2011) Peracetylated 4-fluoro-glucosamine reduces the content and repertoire of *N*- and *O*-glycans without direct incorporation. *J. Biol. Chem.* **286,** 21717–21731

47. Okeley, N. M., Alley, S. C., Anderson, M. E., Boursalian, T. E., Burke, P. J., Emmerton, K. M., Jeffrey, S. C., Klussman, K., Law, C. L., Sussman, D., Toki, B. E., Westendorf, L., Zeng, W., Zhang, X., Benjamin, D. R., and Senter, P. D. (2013) Development of orally active inhibitors of protein and cellular fucosylation. *Proc. Natl. Acad. Sci. U.S.A.* **110,** 5404–5409

Systemic Blockade of Sialylation in Mice with a Global Inhibitor of Sialyltransferases

Matthew S. Macauley, Britni M. Arlian, Cory D. Rillahan, Poh-Choo Pang, Nikki Bortell, Maria Cecilia G. Marcondes, Stuart M. Haslam, Anne Dell and James C. Paulson

Access the most updated version of this article at doi: 10.1074/jbc.M114.606517

Alerts:
- When this article is cited
- When a correction for this article is posted

Click here to choose from all of JBC's e-mail alerts

Supplemental material:
http://www.jbc.org/content/suppl/2014/11/03/M114.606517.DC1

This article cites 45 references, 19 of which can be accessed free at
http://www.jbc.org/content/289/51/35149.full.html#ref-list-1